

# Spherical media and geodesic lenses in geometrical optics

Martin Šarbort and Tomáš Tyc

Institute of Theoretical Physics and Astrophysics, Masaryk University, Kotlářská 2, 61137 Brno, Czech Republic

E-mail: [masicek@centrum.cz](mailto:masicek@centrum.cz) and [tomtyc@physics.muni.cz](mailto:tomtyc@physics.muni.cz)

Received 12 April 2012, accepted for publication 14 June 2012

Published 3 July 2012

Online at [stacks.iop.org/JOpt/14/075705](http://stacks.iop.org/JOpt/14/075705)

## Abstract

This paper presents a general approach to solving the problems of inverse scattering in three-dimensional isotropic media with a spherically symmetric refractive index distribution. It is based on equivalence of the central section of an inhomogeneous medium and corresponding geodesic lens, which is a non-Euclidean surface with constant refractive index. We use this approach for solving the Luneburg inverse problem and also for the derivation and design of absolute instruments that provide perfect imaging within the frame of geometrical optics. In addition, we solve the generalized Luneburg inverse problem, which leads to the discovery of a new class of magnifying lenses.

**Keywords:** spherical medium, geodesic lens, absolute instrument, magnifying lens, inverse scattering, perfect imaging, geometrical optics

(Some figures may appear in colour only in the online journal)

## 1. Introduction

In recent years there has been great progress in research into three-dimensional isotropic spherical media, i.e. media with a spherically symmetric distribution of refractive index. These media can be treated within the frame of geometrical optics as two-dimensional, because each propagating light ray lies in a plane through the center of symmetry. This feature greatly simplifies physical considerations, as well as their mathematical description.

Spherical media have a long history, having first been described by James Clerk Maxwell in 1854 (Maxwell's fish-eye). Much of the research in this field was done in terms of geometrical optics in the mid-twentieth century. First, Luneburg [1] solved the inverse scattering problem for spatially limited spherical media and derived the refractive index of the lens which focuses a beam of parallel rays into a point on its opposite surface. Then Eaton [2] found another lens which works as an omni-directional retroreflector, and about the same time Firsov [3] discussed the problem of perfectly focusing spherical media, called later absolute instruments [4]. This work was recently followed by Miñano [5], who dealt with perfect imaging in homogeneous

three-dimensional regions, and Tyc *et al* [6], who described a general method for the design of absolute instruments that provide perfect imaging within geometrical optics.

The extraordinary properties of the Luneburg and Eaton lenses found possible applications in opto-electronics shortly after their discovery. However, a big problem emerged—the inability to produce a non-homogeneous distribution of refractive index. A solution was found by Rinehart [7], who replaced the central sections of spherical lenses by equivalent curved two-dimensional surfaces with rotational symmetry and constant refractive index, which was easy to achieve. The light rays confined to these surfaces propagate along the geodesics, hence the curved surfaces were called geodesic lenses. Their properties were later studied by many researchers [8–11], but mostly in connection with the Luneburg inverse problem. Recently, geodesic lenses have found applications in non-imaging optics [12].

In this paper we deal with isotropic spherical media in terms of geometrical optics. This allows us to reduce the description to two dimensions and employ the concept of equivalent geodesic lenses that would be hard to imagine for three-dimensional media. We show that this concept is advantageous for solving the Luneburg inverse problem, as

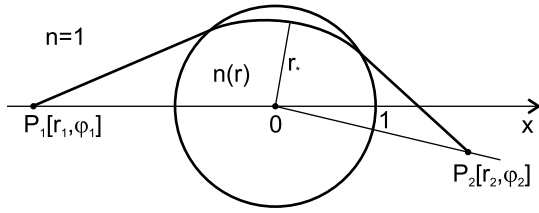


**Figure 1.** Geometrical configuration of the Luneburg inverse problem.

well as for the derivation and analysis of absolute instruments. In addition, we use the idea of a geodesic lens for solving the generalized Luneburg inverse problem discussed in [13–15], which will lead us to the discovery of a new class of magnifying lenses.

The paper is organized as follows. In section 2 we state the Luneburg problem and find its solution using the concept of a geodesic lens. In section 3 we generalize the idea of a geodesic lens and use it for design of absolute instruments that provide perfect imaging within the frame of geometrical optics. In section 4 we deal with the generalized Luneburg problem. Section 5 concludes the paper.

## 2. The Luneburg problem and geodesic lenses

In this section we first formulate the Luneburg inverse problem. Then we introduce the concept of a geodesic lens and we use it to solving the given problem.

### 2.1. The Luneburg problem

Let us consider the system of polar coordinates  $(r, \varphi)$  in a plane and a lens of unit radius with the center at the origin (see figure 1). The refractive index inside the lens is described by a spherically symmetric function  $n(r)$  which fulfills the condition  $n(1) = 1$ ; outside the lens the refractive index is set to unity. Next, suppose that all the light rays which emerge from a point source  $P_1[r_1, \varphi_1]$  in the direction of decreasing  $\varphi$  and which pass through the lens meet at the point  $P_2[r_2, \varphi_2]$ , where a real image of the source is formed. Then the Luneburg inverse problem lies in the derivation of the unknown refractive index  $n(r)$  from the knowledge of the source and image coordinates.

A solution of this inverse problem utilizes the well-known analogy between classical mechanics and geometrical optics. This implies that a light ray trajectory in the spherical medium is characterized by a constant value of the quantity  $L$ , which corresponds to an angular momentum known from classical mechanics. It is given by

$$L = rn(r) \sin \alpha, \tag{1}$$

where  $\alpha$  is an angle between the ray trajectory and radius vector (see figure 2). We will call the quantity  $L$  simply angular momentum. In addition, the point of the ray trajectory where  $\alpha = \pi/2$  will be referred to as a turning point and its radial coordinate as  $r_*$ . The line element  $dl$  of the ray trajectory, shown in figure 2, can be expressed as  $dl =$

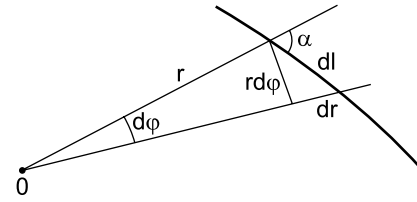


**Figure 2.** Ray path in a spherical medium.

$r d\varphi / \sin \alpha$  or  $dl^2 = dr^2 + r^2 d\varphi^2$ . Using these relations, together with equation (1), we obtain the differential equation that describes the ray trajectory in a spherical medium

$$d\varphi = \pm \frac{L dr}{r\sqrt{n^2 r^2 - L^2}}. \tag{2}$$

This equation can now be used in the Luneburg problem. Denoting the total change of polar angle swept by the light ray during its propagation from the source to the image by  $-M\pi$  ( $M$  is a nonnegative real number), we get for the ray drawn in figure 1 the equation

$$-M\pi = \int_{r_1}^1 \frac{L dr}{r\sqrt{n^2 r^2 - L^2}} - 2 \int_{r_*}^1 \frac{L dr}{r\sqrt{n^2 r^2 - L^2}} - \int_1^{r_2} \frac{L dr}{r\sqrt{n^2 r^2 - L^2}}. \tag{3}$$

The first and third terms on the right-hand side correspond to the propagation of the ray outside the lens where  $n = 1$ , while the second term corresponds to the propagation through the lens with refractive index  $n(r)$ . The first and third terms can be easily evaluated, and after rearrangement we get an integral equation for the function  $n(r)$

$$\int_{r_*}^1 \frac{L dr}{r\sqrt{n^2 r^2 - L^2}} = \frac{1}{2} \left( M\pi + \arcsin \frac{L}{r_1} + \arcsin \frac{L}{r_2} - 2 \arcsin L \right). \tag{4}$$

The standard procedure for solving this integral equation and calculation of an unknown refractive index  $n(r)$  can be found in [1]. Here we proceed by a different method, employing the concept of geodesic lenses.

### 2.2. The Luneburg problem and geodesic lenses

Another method of solving the Luneburg problem lies in the replacement of the inhomogeneous lens with refractive index  $n(r)$  considered before with an equivalent geodesic lens which is a curved two-dimensional surface (waveguide) with rotational symmetry and refractive index set to unity (see figure 3). Therefore, we first calculate the shape of the geodesic lens and consequently the desired refractive index  $n(r)$ . It should be emphasized that the equivalence of the inhomogeneous lens and geodesic lens is based on a simple requirement—the corresponding optical path elements must be the same.

Let us first introduce the coordinates that determine the shape of the geodesic lens whose axis of symmetry is identical

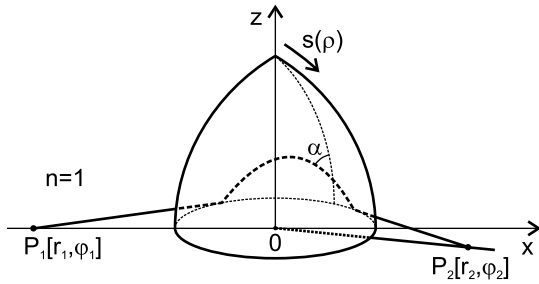


**Figure 3.** Geometrical configuration of the Luneburg inverse problem with a geodesic lens.

to the  $z$  axis shown in figure 3. Each point of the geodesic lens is described by a radial coordinate  $\rho$ , angular coordinate  $\theta$  and a value of function  $s(\rho)$ , which represents the length of the surface measured along the meridian from the axis of symmetry to the given point (see figure 3).

The coordinate transformation between the inhomogeneous lens with refractive index  $n(r)$  and the geodesic lens follows from the requirement for equivalence of the corresponding optical path elements. For the inhomogeneous lens the square of optical path element is  $d\sigma^2 = n^2(dr^2 + r^2 d\varphi^2)$ ; for a geodesic lens we state  $d\sigma^2 = ds^2 + \rho^2 d\theta^2$ . Assuming  $\theta = \varphi$ , we get from the comparison of corresponding path elements

$$\rho = nr, \quad ds = n dr. \tag{5}$$

These relations completely determine the conformal mapping between the inhomogeneous lens and the equivalent geodesic lens. For the rest of this section we will assume that  $\rho(r)$  is an increasing function with a single maximum at  $r = 1$ .

As a consequence of (5) we can write the angular momentum  $L$  that characterizes the ray trajectory on geodesic lens as

$$L = \rho \sin \alpha, \tag{6}$$

where  $\alpha$  is an angle between the ray trajectory and the meridian (see figure 3). Using the coordinate transformation (5) we can also rewrite (2) and we obtain the differential equation that describes the ray trajectory on the geodesic lens

$$d\theta = \pm \frac{Ls'(\rho) d\rho}{\rho\sqrt{\rho^2 - L^2}}, \tag{7}$$

where  $s'(\rho) = ds(\rho)/d\rho$ . The same coordinate transformation applied on (4) gives us

$$\int_L^1 \frac{Ls'(\rho)d\rho}{\rho\sqrt{\rho^2 - L^2}} = \frac{1}{2} \left( M\pi + \arcsin \frac{L}{r_1} + \arcsin \frac{L}{r_2} - 2 \arcsin L \right), \tag{8}$$

which is an integral equation for the derivative of unknown function  $s(\rho)$  that determines the shape of the geodesic lens in the Luneburg inverse problem. After calculating this function we will be able to find the refractive index  $n(r)$ .

### 2.3. Solution of the Luneburg problem with a geodesic lens

In fact, the integral equation (8) is a kind of Abel integral equation, which can be solved by a slight modification of the method described in detail in [6]. Due to the length of the general solution itself we omit it here and we write the final result for the function  $s(\rho)$  which we have derived for the first time in the form

$$s(\rho) = -\frac{1}{\pi} \left[ \rho \arcsin \sqrt{\frac{1 - \rho^2}{r_1^2 - \rho^2}} + \rho \arcsin \sqrt{\frac{1 - \rho^2}{r_2^2 - \rho^2}} + r_1 \arcsin \left( \rho \sqrt{\frac{r_1^2 - 1}{r_1^2 - \rho^2}} \right) + r_2 \arcsin \left( \rho \sqrt{\frac{r_2^2 - 1}{r_2^2 - \rho^2}} \right) - \sqrt{r_1^2 - 1} \arcsin \rho - \sqrt{r_2^2 - 1} \arcsin \rho - \arcsin \frac{1}{r_1} \arcsin \rho - \arcsin \frac{1}{r_2} \arcsin \rho \right] + (M - 1) \arcsin \rho + \rho. \tag{9}$$

We see that for general positions of the source  $P_1[r_1, \varphi_1]$  and image  $P_2[r_2, \varphi_2]$  the shape of the geodesic lens is given by a very complicated formula.

Let us now study some special cases. The function  $s(\rho)$  given by (9) becomes very simple when the values of coordinates  $r_1, r_2$  are delimited to only two possibilities—unity and infinity. Then the function  $s(\rho)$  can be written in a simplified form

$$s(\rho) = A\rho + B \arcsin \rho, \tag{10}$$

where  $A$  and  $B$  are real constants given by

$$A = 1 - \frac{1}{\pi} \arcsin \sqrt{\frac{1 - \rho^2}{r_1^2 - \rho^2}} - \frac{1}{\pi} \arcsin \sqrt{\frac{1 - \rho^2}{r_2^2 - \rho^2}} \tag{11}$$

$$B = (M - 1) + \frac{1}{\pi} \arcsin \frac{1}{r_1} + \frac{1}{\pi} \arcsin \frac{1}{r_2}. \tag{12}$$

The simplified formula (10) was first proposed in [8], but only as a generalization of the function that describes the shape of a geodesic lens equivalent to a Luneburg lens. Therefore the relations (11) and (12) between the numbers  $A, B$  and the coordinates of the source and image have been unknown so far. Now, it is obvious that the number  $A$  has only three possible values,  $0, \frac{1}{2}$  and  $1$ , which correspond to three different situations: respectively, both the source and image are placed on the unit circle, one of these points is on the unit circle and the second point is at infinity, both of these points are at infinity. Moreover, since the terms  $\sqrt{(1 - \rho^2)/(r^2 - \rho^2)}$  and  $1/r$  equal each other for  $r$  delimited to unity and infinity, adding the equations (11) and (12) gives the relation  $A + B = M$ .

The geometric meaning of numbers  $A, B$ , which has also not yet been fully understood, becomes clear when we calculate the total change of polar angle  $\Delta\theta_{gl}$  swept on the geodesic lens by the ray with angular momentum  $L$ . We get

$$\Delta\theta_{gl}(L) = 2 \int_L^1 \frac{Ls'(\rho) d\rho}{\rho\sqrt{\rho^2 - L^2}} = (A + B)\pi - 2A \arcsin L. \tag{13}$$

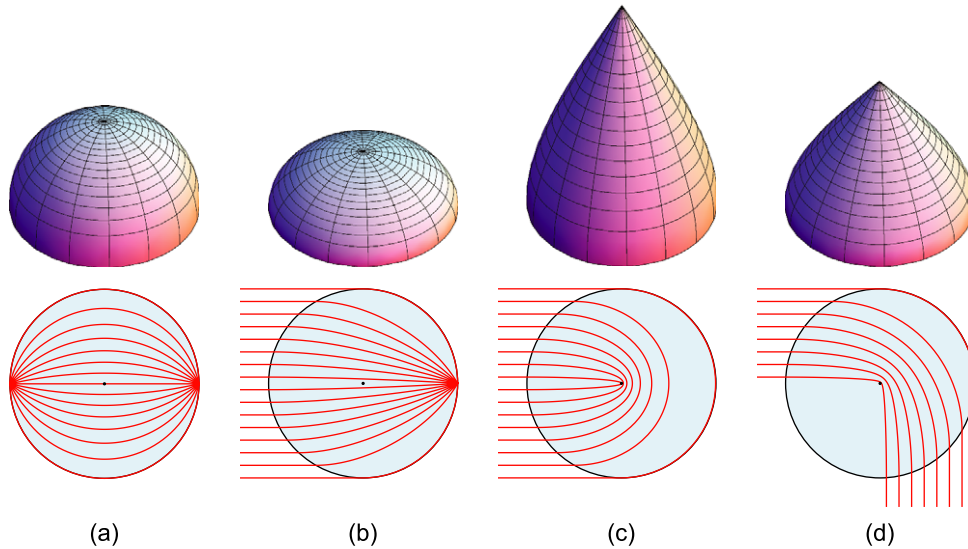


**Figure 4.** Ray tracing and equivalent geodesic lenses for several solutions of the Luneburg problem: (a) Maxwell's fish-eye, (b) Luneburg lens, (c) Eaton lens, (d) 90° rotating lens. The spherical medium is shown in light blue.

**Table 1.** Geometric parameters and refractive indices of known lenses.

Lens	$r_1$	$r_2$	$M$	$A$	$B$	Refractive index
Maxwell's fish-eye	1	1	1	0	1	$n(r) = \frac{2}{1+r^2}$
Generalized Maxwell's fish-eye	1	1	$M$	0	$M$	$n(r) = \frac{2r^{1/M-1}}{1+r^{2/M}}$
Luneburg	1	$\infty$	1	$\frac{1}{2}$	$\frac{1}{2}$	$n(r) = \sqrt{2-r^2}$
Beam divider (point source)	1	$\infty$	$M$	$\frac{1}{2}$	$M - \frac{1}{2}$	
Plane	$\infty$	$\infty$	1	1	0	$n(r) = 1$
90° rotating	$\infty$	$\infty$	$\frac{3}{2}$	1	$\frac{1}{2}$	$rn^4 - 2n + r = 0$
Eaton	$\infty$	$\infty$	2	1	1	$n(r) = \sqrt{\frac{2}{r} - 1}$
Invisible	$\infty$	$\infty$	3	1	2	$rn^{3/2} + nr^{1/2} - 2 = 0$
Beam divider (parallel ray source)	$\infty$	$\infty$	$M$	1	$M - 1$	

We see that the ray with  $L = 1$ , which hits the circle  $\rho = 1$  in a tangential direction (and therefore propagates on the geodesic lens along this circle), sweeps the angle  $B\pi$  on geodesic lens. As a consequence, the total polar angle swept by the same ray in the plane around the geodesic lens is  $A\pi$ . This geometric interpretation of numbers  $A, B$  is very important, since it allows us to deduce the shape of the geodesic lens very quickly from the behavior of light rays. One can check these results on several examples of known lenses shown in figure 4; the discussed parameters are also summarized for other lenses in table 1.

The parametrization of a geodesic lens by the function  $s(\rho)$  proved very advantageous in the previous description. However, for the real construction of a geodesic lens it is better to describe its shape with the function  $z(\rho)$  rather than  $s(\rho)$ . These functions are related by the equation  $dz^2 = ds^2 -$

$d\rho^2$ , and for function  $s(\rho)$  given by (10) we obtain

$$dz = \pm \left[ \left( A + \frac{B}{\sqrt{1-\rho^2}} \right)^2 - 1 \right]^{1/2} d\rho. \quad (14)$$

It is apparent that the geodesic lens can be constructed only if the condition  $|A + B| \geq 1$  holds. For  $A + B = 1$  the geodesic lens has a flat top, otherwise there is a sharp tip on the top. These properties are apparent in figure 4, where several examples of geodesic lenses are shown.

#### 2.4. Calculation of refractive index $n(r)$ from the function $s(\rho)$

Once we have the function  $s(\rho)$  given by (10) that describes the shape of the geodesic lens, we can calculate the refractive index  $n(r)$  of the corresponding inhomogeneous lens [9]. Using the relations  $ds = n dr$  and  $\rho = nr$  we can write

$$\frac{dr}{r} = s'(\rho) \frac{d\rho}{\rho} = \left( A + \frac{B}{\sqrt{1-\rho^2}} \right) \frac{d\rho}{\rho}. \quad (15)$$

With substitution  $\rho = \sin \gamma$ , the integration gives

$$\ln r = A \ln \rho + B \ln \left( \tan \frac{\gamma}{2} \right) + B \ln f, \quad (16)$$

where the last term on the right-hand side represents the integration constant, and  $f$  is a real positive number. After rearrangement and use of the requirement  $\rho(1) = 1$  imposed earlier we get  $f = 1$ . Then we obtain the final equation

$$r^{2/B} - 2r^{1/B} (nr)^{A/B-1} + (nr)^{2A/B} = 0, \quad (17)$$

which was first derived in [9], but without clear connection to the Luneburg problem. From this formula the refractive index  $n(r)$  can be calculated for given parameters  $A$  and  $B$ ; the results for several known lenses are summarized in table 1. In general, for  $A + B = 1$  we get the finite value of refractive

index at the origin which corresponds to a flat top geodesic lens. Otherwise the refractive index goes to infinity at the origin, which corresponds to a sharp tip on the top of a geodesic lens.

Let us now summarize the results of this section. Using the concept of a geodesic lens we found the general solution of the Luneburg inverse problem. Consequently, we derived the simplified function (10) that, so far, all authors used as a prerequisite and we explained the geometric meaning of numbers  $A, B$  in detail. These results are going to be very useful in the following section aiming to the derivation of spherical media called absolute instruments.

### 3. Absolute instruments and geodesic lenses

In this section we first deal with an inverse scattering problem in a general spherical medium which meets certain conditions. As before, we use for its solution the concept of an equivalent geodesic lens. Then we apply the general results for derivation of spherical media that behave as absolute instruments, i.e. provide perfect imaging within the frame of geometrical optics.

#### 3.1. A general spherical medium and a geodesic lens

Let us start with a general spherical medium with refractive index  $n(r)$  defined in a circular region of radius  $R > 1$  and satisfying the following conditions. We assume that the corresponding function  $\rho(r) = m(r)$  has a single global maximum  $\rho(1) = 1$ , the value  $\rho(0) = 0$  and  $\lim_{r \rightarrow R} \rho(r) = 0$ . Clearly, these assumptions imply that the inverse function  $r(\rho)$  is multivalued; we denote the two corresponding branches  $r_{\pm}(\rho)$ .

As we know from the previous section, the light ray characterized by angular momentum  $L$  given by (1) can propagate in the spherical medium only in the region where  $L \leq \rho(r)$ . Therefore, in the medium which satisfies the above assumptions the ray trajectory is spatially confined to the annulus with inner radius  $r_-(L)$  and outer radius  $r_+(L)$ . The turning points lie on both circular boundaries of this annulus. We denote by  $\Delta\varphi_{tp}(L)$  a polar angle swept by the light ray during the propagation between two consecutive turning points. Then the inverse scattering problem lies in the derivation of the unknown refractive index  $n(r)$  from the given function  $\Delta\varphi_{tp}(L)$ .

To solve such a problem we utilize the concept of a geodesic lens. Similarly to before, we use the conformal mapping (5) for representation of the considered spherical medium by an equivalent geodesic lens. Its general shape results from the above conditions imposed on the function  $\rho(r)$ , and it is sketched in figure 5(a). The circle  $\rho = 1$ , called an equator, corresponds to the circle  $r = 1$  in the spherical medium and divides the geodesic lens into two parts. To maintain consistency with the previous section we assume that the upper and lower parts of geodesic lens correspond in the spherical medium to the region inside and outside the unit circle, respectively. Then the intersections  $T_1$  and  $T_2$  of the

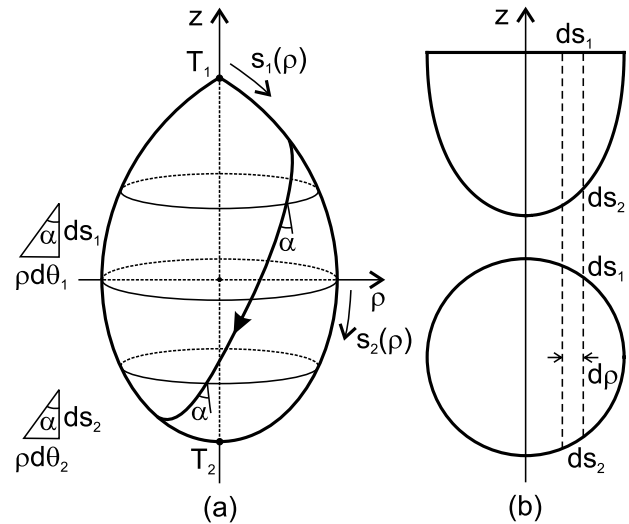


**Figure 5.** (a) General geodesic lens. (b) Reshaping of an asymmetrical geodesic lens into a symmetrical one.

geodesic lens with the  $z$  axis correspond to the point  $r = 0$  and the circle  $r = R$ , respectively.

It is obvious from this spatial arrangement that in general there are two different points with the same value of radius  $\rho$  and angle  $\theta$ , but with different length  $s(\rho)$  values defined in section 2. For the distinction of these two points we describe the geodesic lens by two branches of the function  $s(\rho)$ . The first branch  $s_1(\rho)$  is measured from the point  $T_1$ , where  $s_1(0) = 0$ , along the meridian to the equator, where it has the value  $s_1(1)$ . The second branch  $s_2(\rho)$  is measured from the equator to the point  $T_2$ , while  $s_2(1) = s_1(1)$  and  $s_2(0) > s_2(1)$ .

Equipped with these definitions we can describe the trajectory of the light ray with angular momentum  $L$  given by (6). Such a ray propagates on the geodesic lens within a region bounded by two circles of radius  $\rho = L$ , one above and one below the equator, on which the turning points are located. A polar angle  $\Delta\theta_{tp}$  swept on the geodesic lens by the light ray during its propagation between two consecutive turning points is given by

$$\Delta\theta_{tp}(L) = \int_L^1 \frac{L s'_1(\rho) d\rho}{\rho \sqrt{\rho^2 - L^2}} + \int_1^L \frac{L s'_2(\rho) d\rho}{\rho \sqrt{\rho^2 - L^2}}, \quad (18)$$

since each of these points lies on the other side of the equator. This formula can be used to solve the inverse scattering problem because for given  $\Delta\theta_{tp}(L)$  it represents an integral equation for functions  $s'_1(\rho)$  and  $s'_2(\rho)$  that describe the shape of the geodesic lens. Nevertheless, it seems impossible to obtain two unknown functions from a single equation.

#### 3.2. Reshaping of a geodesic lens

The integral equation (18) can be solved if we realize one important property of geodesic lenses which satisfies the conditions stated for function  $\rho(r)$ . Between two consecutive turning points the light ray with angular momentum  $L$  crosses on the geodesic lens two different circles with the same value of radius  $\rho > L$  but different values  $s_1(\rho)$  and  $s_2(\rho)$  (see

figure 5(a)). Clearly, at both intersection points the trajectory makes the same angle  $\alpha$  with the local meridian. Using these facts and the geometric configuration shown in figure 5(a) we can write the sum of infinitesimal changes of polar angle at the two intersection points as  $d\theta_1 + d\theta_2 = \frac{\tan \alpha}{\rho}(ds_1 + ds_2)$ , where the differentials  $ds_1, ds_2$  have the same sign, since they are measured in the same direction along the ray trajectory. We see that if we change the shape of the geodesic lens in such a way that  $ds_1 + ds_2$  remains unchanged for given  $\rho$ , the sum  $d\theta_1 + d\theta_2$  also remains unchanged. This property holds for arbitrary  $\rho$ , hence we can change the shape of a geodesic lens without changing the total polar angle  $\Delta\theta_{tp}$  swept by the light ray during its propagation between two consecutive turning points.

To describe the reshaping of a geodesic lens we use the differentials  $ds_1, ds_2$  in the sense introduced above, i.e. with respect to the trajectory of a particular light ray. For definiteness, we assume that the reference ray propagates on the geodesic lens from the upper to the lower part, hence the differentials  $ds_1, ds_2$ , as well as all the similar differentials introduced later, are positive.

An important option of reshaping the geodesic lens is shown in figure 5(b), where we consider the central section of a geodesic lens which is asymmetrical with respect to the equatorial plane. By changing its shape within the stripes of infinitesimal width  $d\rho$  in order to keep the sum  $ds_1 + ds_2$  unchanged, we obtain another geodesic lens which is symmetrical with respect to the equatorial plane. As such a transformation can be performed with each geodesic lens, it is natural to write

$$ds_1 = ds_s + ds_a, \quad ds_2 = ds_s - ds_a, \quad (19)$$

where  $ds_s$  describes the symmetric part of the geodesic lens, while  $ds_a$  describes the antisymmetric part. Using this notation we rewrite the integral equation (18) as

$$\Delta\theta_{tp}(L) = 2 \int_L^1 \frac{L s'_s(\rho) d\rho}{\rho \sqrt{\rho^2 - L^2}}, \quad (20)$$

since the terms with  $s'_a(\rho)$  are mutually subtracted. For given  $\Delta\theta_{tp}(L)$  we can solve this integral equation and find the shape of a symmetrical geodesic lens described by functions  $s_1(\rho) = s_s(\rho)$  and  $s_2(\rho) = 2s_s(1) - s_s(\rho)$ . Then, by choosing the differential  $ds_a$ , we can make the geodesic lens asymmetrical in an almost arbitrary way, still maintaining the desired form of  $\Delta\theta_{tp}(L)$ . Consequently, from the different shapes of geodesic lenses we can find a variety of refractive indices.

### 3.3. Absolute instruments and geodesic lenses

Let us now apply the general method for solving the inverse scattering problem to derivation of a specific type of spherical medium called absolute instruments. These provide perfect imaging in the sense of geometrical optics, which can be achieved if the trajectories of all possible rays are closed.

In the simplest case the requirement of closed trajectories means that the polar angle  $\Delta\theta_{tp}$  swept by the light ray during

the propagation between two consecutive turning points does not depend on angular momentum  $L$  and can be written as

$$\Delta\theta_{tp} = K\pi, \quad (21)$$

where  $K$  is a rational number that is the inverse of the number  $m$  used in [6]. Inserting this expression into (20) we obtain an integral equation for the function  $s'_s(\rho)$  which describes the shape of a symmetrical geodesic lens that provides perfect imaging.

A solution of this integral equation can be found by a slight modification of the method presented in [6], therefore we omit it here due to its length. As a final result, we get the function

$$s_s(\rho) = K \arcsin \rho. \quad (22)$$

However, this is formally identical to  $B \arcsin \rho$ , which is the second term on the right-hand side of (10) obtained as a simplified solution of the Luneburg inverse problem. Hence we can use the results of section 2 for analysis of the function (22). We see that for  $K = 1$  the function (22) describes the unit sphere, which is a geodesic representation of the well-known Maxwell's fish-eye (see table 1). For general  $K$  the symmetrical geodesic lens corresponds to generalized Maxwell's fish-eye [6].

Once we have the symmetrical geodesic lens given by the function  $s_s(\rho)$ , we can reshape it according to (19) by choosing the function  $s_a(\rho)$ , while the sum  $ds_1 + ds_2$ , rewritten as

$$ds_1 + ds_2 = 2 ds_s = \frac{2K}{\sqrt{1 - \rho^2}} |d\rho|, \quad (23)$$

must hold. Obviously, we can choose the function  $s_a(\rho)$  which makes the geodesic lens asymmetrical in infinitely many ways. This fact represents in another way the freedom in designing the absolute instruments discussed in [6]. In the remainder of this section we describe several interesting options of reshaping of a geodesic lens.

### 3.4. Absolute instruments and the Luneburg problem

Looking back to section 2 we see that we have already found one option for function  $s_a(\rho)$  as a solution of the Luneburg problem—from (10) we have  $s_a(\rho) = A\rho$ . Then the geodesic lens is described by the functions

$$\begin{aligned} s_1(\rho) &= A\rho + K \arcsin \rho, \\ s_2(\rho) &= A\rho + K(\pi - \arcsin \rho). \end{aligned} \quad (24)$$

The corresponding refractive index of the absolute instrument can be calculated using (17), while  $B = \pm K$ . Since (17) is invariant with respect to the change  $B \rightarrow -B$ , we obtain the same functional dependence  $n(r)$  from both  $s_1(\rho)$  and  $s_2(\rho)$ . For given  $A, K$  we find the same functions  $n(r)$  which are already summarized in table 1, but now the refractive index fills the whole circular area of radius  $R$  and not only the unit circle. The ray tracing for several examples is shown in figure 6.

As in section 2, it is also interesting to discuss the conditions that must be met in order to construct the entire

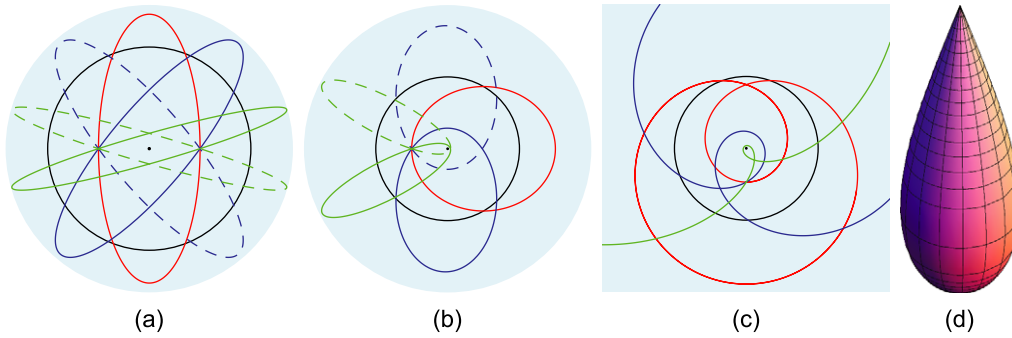


**Figure 6.** Ray trajectories in absolute instruments represented by spherical media with refractive indices of (a) a Luneburg, (b) an Eaton and (c) an invisible lens. The black circle corresponds to the circular trajectory at  $r = 1$  with maximum possible angular momentum. (d) Geodesic lens equivalent to the spherical medium with the refractive index of an invisible lens.

geodesic lens. The calculation of the corresponding functions  $z_1(\rho)$  and  $z_2(\rho)$  gives us the conditions  $|A + K| \geq 1$  and  $|A - K| \geq 1$  for the upper and lower part of geodesic lens, respectively. For example, both these conditions are satisfied for  $A = 0, K = 1$  that corresponds to a sphere which is a geodesic representation of Maxwell’s fish-eye. The next example is for the choice  $A = 1, K = 2$  which corresponds to the refractive index of an invisible lens; the geodesic lens is shown in figure 6(d). As an example for which the second condition is not satisfied and, therefore, the lower part of a geodesic lens cannot be completely constructed, we can take  $A = 1, K = 1$  which corresponds to the refractive index of an Eaton lens.

3.5. Absolute instruments with a region of constant refractive index

Another class of absolute instruments which might be useful in practical applications are absolute instruments with a circular region of constant refractive index. We show now that these can be very simply designed using the formula (23).

First, it is important to realize that in the region of constant refractive index the function  $\rho(r)$  monotonically increases. This implies that the homogeneous region must lie inside the unit circle, since we need to fulfill the conditions stated for the function  $\rho(r)$  at the beginning of this section. For simplicity, let us assume that the homogeneous region fills the whole unit circle.

Then for the upper part of the geodesic lens which corresponds to the homogeneous region we obtain from transformation (5) the relation  $ds_1 = |d\rho|$ . Inserting this into (23) we calculate the differential  $ds_2$  which must be chosen to achieve the properties of absolute instruments. We get

$$ds_1 = |d\rho|, \quad ds_2 = -|d\rho| + \frac{2K}{\sqrt{1-\rho^2}}|d\rho|, \quad (25)$$

which leads to

$$s_1(\rho) = \rho, \quad s_2(\rho) = \rho + 2K \left( \frac{\pi}{2} - \arcsin \rho \right). \quad (26)$$

The refractive indices which correspond to these functions can be easily calculated from (17). For  $s_1(\rho)$  we have  $A = 1, B = 0$ , which corresponds to the unit refractive index inside

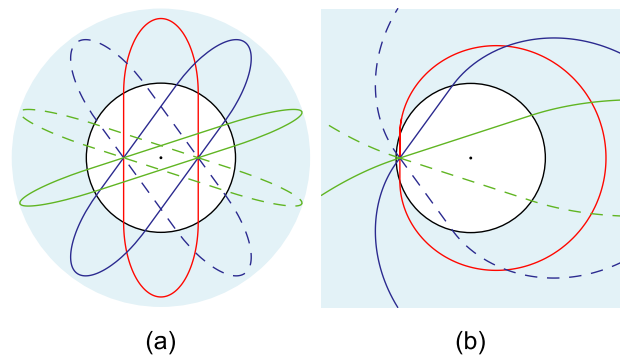


**Figure 7.** Ray trajectories in absolute instruments with a region of constant refractive index which is shown in white: (a) inverse Eaton lens, (b) inverse invisible lens.

the unit circle. For  $s_2(\rho)$  we have  $A = 1, B = 2K$ , which means that the homogeneous region can be accompanied by infinitely many different media through which we achieve the properties of absolute instruments. So far, only two such examples are known—when  $K = \frac{1}{2}$  the refractive index is given by the formula that describes the Eaton lens, for  $K = 1$  the refractive index corresponds to an invisible lens. These two absolute instruments were first introduced in [5] and were called an inverse Eaton lens (or later a Miñano lens [6]) and an inverse invisible lens; they are shown in figure 7.

3.6. Absolute instruments with a mirror boundary

Until now, we have studied absolute instruments whose refractive index was given by one function in the whole circular area of radius  $R$  or by two different functions inside and outside the unit circle, respectively. These were obtained by reshaping the symmetrical geodesic lens by function  $s_a(\rho)$  common for all  $\rho$ .

However, we can also choose the function  $s_a(\rho)$  in a different way for various subintervals of  $\rho \in [0, 1]$ . Since each subinterval of  $\rho$  corresponds on a geodesic lens to two circular stripes, one of which lies above and one below the equatorial plane, we obtain the spherical medium divided into pairs of annular rings, one of which lies inside and one outside the unit circle. The refractive indices in the rings of each pair

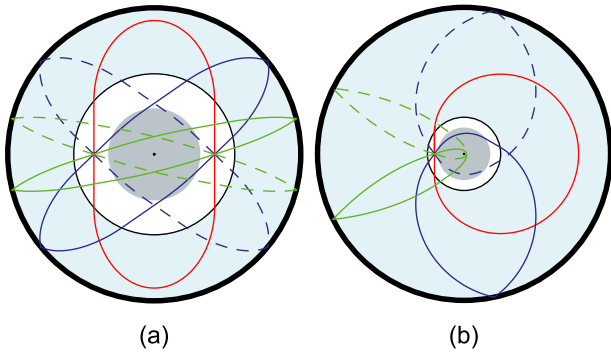


**Figure 8.** Ray trajectories in absolute instruments with a region of constant refractive index and mirror boundary: (a) inverse Eaton lens, (b) inverse invisible lens. The central region with the refractive index of an appropriate Maxwell's fish-eye, which compensates the effect of mirror, is shown in darker blue.

are mutually complementary with respect to the relation (23), through which the spherical medium achieves the properties of an absolute instrument.

Showing several examples, we restrict ourselves to two subintervals of  $\rho$  denoted as  $[0, \rho_m]$  and  $[\rho_m, 1]$ , to which two functions  $s_{a1}(\rho)$  and  $s_{a2}(\rho)$  correspond, respectively. To maintain consistency in the notation we also split the function  $s_1(\rho)$  into two functions  $s_{11}(\rho)$  and  $s_{12}(\rho)$  which describe the upper part of a geodesic lens gradually from the top to the equator. Similarly, the functions  $s_{22}(\rho)$  and  $s_{21}(\rho)$  describe the lower part of a geodesic lens gradually from the equator downwards. Then the equivalent spherical medium is divided into four annular regions numbered by indices of functions  $s_{ij}(\rho)$ , i.e. the regions are numbered 11, 12, 22 and 21 sequentially from the origin.

In the examples that we would like to show, the particular choice of  $s_{a1}(\rho)$  is motivated by the following consideration. The absolute instruments which fulfill the properties stated for function  $\rho(r)$  at the beginning of this section have one common property. Since we assumed  $\lim_{r \rightarrow R} \rho(r) = 0$ , the refractive index decreases to zero for  $r \rightarrow R$ . Therefore, the ratio of maximum and minimum values of refractive index becomes infinite. This unpleasant feature can be eliminated by adding a circular mirror on the circle of radius  $1 \leq r_m < R$ . Nevertheless, to maintain the properties of absolute instruments, it is necessary to compensate the effect of the mirror in an appropriate way. Its description becomes very simple when we use the concept of a geodesic lens.

We just need to realize that the mirror placed on a geodesic lens at the lower circle of radius  $\rho_m = \rho(r_m)$  means that  $ds_{21} = 0$ . Then we obtain  $ds_{a1} = K/\sqrt{1 - \rho^2}|d\rho|$  which gives us

$$ds_{11} = \frac{2K}{\sqrt{1 - \rho^2}}|d\rho|, \quad ds_{21} = 0. \quad (27)$$

We see that the refractive index in the region 11 which compensates the effect of the mirror corresponds to the generalized Maxwell's fish-eye with  $B = 2K$ . This is a general result that does not depend on the choice of function  $ds_{a2}$  which determines the functions  $s_{12}(\rho)$ ,  $s_{22}(\rho)$  and,

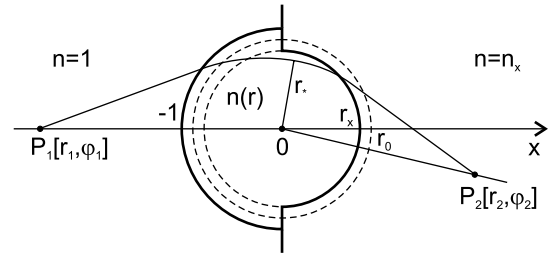


**Figure 9.** Geometric configuration of the generalized Luneburg problem.

consequently, the refractive indices in the regions 12 and 22. However, it should be emphasized that the refractive index of a generalized Maxwell's fish-eye is not given simply by the function listed in table 1 but it must be calculated from (17) for an appropriate value of the integration parameter  $f$ , which makes the refractive index continuous on the boundary of regions 11 and 12.

Since the absolute instruments of particular interest are those with the region of constant refractive index discussed above, we choose  $ds_{a2} = |d\rho| - K/\sqrt{1 - \rho^2}|d\rho|$ . Then for regions 12 and 22 we obtain the same refractive indices as in the section 3.5 for the region inside and outside the unit circle, respectively. Two examples of absolute instruments with a mirror boundary for  $K = \frac{1}{2}$  and 1 are shown in figure 8; the former was recently proposed in [6] while the latter is presented for the first time.

To summarize this section we can say that using the concept of a geodesic lens we found a powerful method for designing and analyzing absolute instruments. The geodesic lenses described by (24) are going to play an important role in the next section aimed at solving another, more general inverse scattering problem.

#### 4. The generalized Luneburg problem and geodesic lenses

In this section we use the concept of a geodesic lens for solving the generalized Luneburg problem, which represents a modification of the problem stated in section 2 that we have not considered yet.

##### 4.1. The generalized Luneburg problem

A geometrical configuration of the generalized Luneburg problem is apparent from figure 9. As before, the light rays emerge from a point source  $P_1$  and propagate through the area of unit refractive index to the unit circle which represents a boundary of the spherical medium with refractive index  $n(r)$ , satisfying the condition  $n(1) = 1$ . But, after passing through, the light rays leave the spherical medium at the circular boundary of radius  $r_x < 1$  where the refractive index is  $n_x = n(r_x)$ . Then the light rays propagate through the area of constant refractive index  $n_x$  to the point  $P_2$  where a real image is formed.

The nature of inverse problem remains the same as before—we would like to deduce the unknown refractive



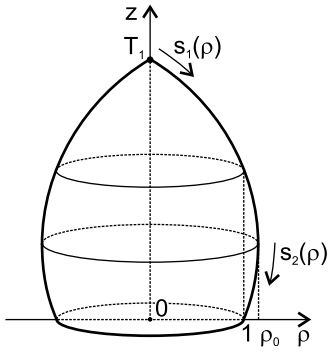


**Figure 10.** Geodesic lens equivalent to the spherical medium in the generalized Luneburg problem.

index  $n(r)$  from given source and image coordinates, while we impose certain conditions on the function  $\rho(r) = m(r)$ . First, we assume that the values of  $\rho(r)$  at the boundaries of spherical media are the same and equal to one. This gives us a relation  $n_x r_x = 1$  for the second boundary. Next, we assume that the function  $\rho(r)$  has a single maximum  $\rho_0 = \rho(r_0) > 1$ , where  $r_x < r_0 < 1$ , and it is increasing and decreasing for  $r$  belonging to the intervals  $[0, r_0]$  and  $[r_0, 1]$ , respectively.

These assumptions stated for a spherical medium determine in general the shape of the equivalent geodesic lens (see figure 10). The circular boundaries of a spherical medium with radii  $r_x$  and 1 correspond to the upper and lower unit circles on a geodesic lens, respectively. Between them there is an equator with radius  $\rho_0 > 1$  which corresponds to the circle of radius  $r_0$ . As in the previous section, we describe the shape of the geodesic lens above and below the equator by the functions  $s_1(\rho)$  and  $s_2(\rho)$ , respectively.

Provided with the geometrical configuration of the geodesic lens, we can describe the light ray trajectories. In the spherical medium, the light ray with angular momentum  $L \in [0, 1]$  propagates from the first boundary to the turning point and then to the second boundary. The corresponding trajectory on the geodesic lens starts at the lower unit circle described by  $s_2(1)$ , where it comes from the source, continues up across the equator and upper unit circle  $s_1(1)$  to the turning point at the circle  $s_1(L)$ , and then back to the unit circle  $s_1(1)$ . Of course, now it is hard to connect the ray trajectory back to the plane in which the source and image are located. However, for our purposes this is not essential.

#### 4.2. Solution of the generalized Luneburg problem

The discussed inverse problem is mathematically expressed by an integral equation which is similar to (8) but involves two unknown functions  $s_1(\rho)$  and  $s_2(\rho)$ . Although we do not know the general solution, we can rigorously calculate its form at least for special cases which are of particular interest—when the source is located on the unit circle or at infinity, and the image is formed on the circle of radius  $r_x$  or at infinity. While solving the problem, it is necessary to use the trick applied before in the study of absolute instruments, where we expanded the functions  $s_1(\rho)$  and  $s_2(\rho)$  into a symmetrical

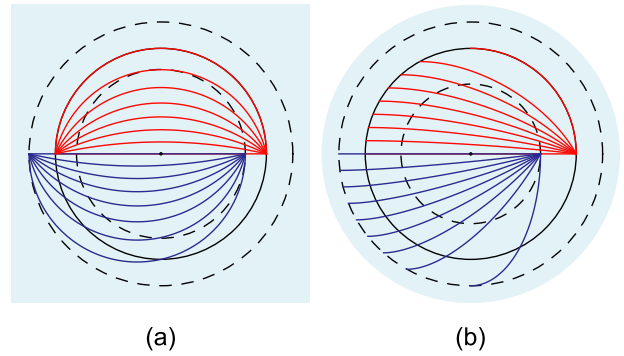


**Figure 11.** Ray trajectories inside the unit circle (red) and between the circles of radii  $r_{\pm}(C)$  (blue) for (a) Maxwell's fish-eye and (b) the Luneburg profile.

and asymmetrical part. Unfortunately, this procedure is quite lengthy.

Instead, the solution can be found easily if we notice one very interesting property of geodesic lenses described by functions (24); for the sake of consistency with section 2 we use  $B$  rather than  $K$ . First, let us recall that in section 2 we calculated the polar angle  $\Delta\theta_{gl}(L)$  swept on the geodesic lens by the light ray with angular momentum  $L$  during the propagation from the equator up to the turning point and back to the equator (see (13)). Exactly on the equator such a ray makes an angle  $\alpha$  with the local meridian. Now, let us consider another ray which makes the same angle  $\alpha$  with the local meridian on the lower circle of radius  $C < 1$  and, therefore, has an angular momentum  $CL$ . When we calculate the polar angle swept on the geodesic lens during its propagation from the lower circle  $s_2(C)$  gradually up to the equator, the upper circle  $s_1(C)$  and the turning point and then back to the upper circle  $s_1(C)$ , we obtain

$$\begin{aligned} \Delta\theta_{gl}(CL) &= \int_C^1 \frac{CL s_2' d\rho}{\rho\sqrt{\rho^2 - C^2 L^2}} + \int_1^{CL} \frac{CL s_1' d\rho}{\rho\sqrt{\rho^2 - C^2 L^2}} \\ &\quad - \int_{CL}^C \frac{CL s_1' d\rho}{\rho\sqrt{\rho^2 - C^2 L^2}} \\ &= (A + B)\pi - 2A \arcsin L. \end{aligned} \tag{28}$$

Surprisingly, the result is independent of  $C$  for arbitrary  $A$ ,  $B$  and, moreover, it is identical to (13). This means that the behavior of light rays characteristic for given  $A$  and  $B$ , which was the essence of solving the Luneburg problem, remains the same for an arbitrary pair of circles with the same radius  $C \in [0, 1]$ . Transformed back to the spherical medium, the characteristic behavior remains the same between the pairs of circles with radii  $r_{\pm}(C)$ . This property has not been known so far, therefore it represents a key result of this section.

The geometrical meaning of this property is shown in figure 11 for two examples. Choosing  $A = 0, B = 1$ , we obtain Maxwell's fish-eye which focuses the light rays coming from the point source located on the unit circle to the image point located on the same circle. If we place the point source on the dashed circle of radius  $r_-(C)$ , the image is formed on the dashed circle of radius  $r_+(C)$ . This property of Maxwell's fish-eye is well known and is linked to the fact that its

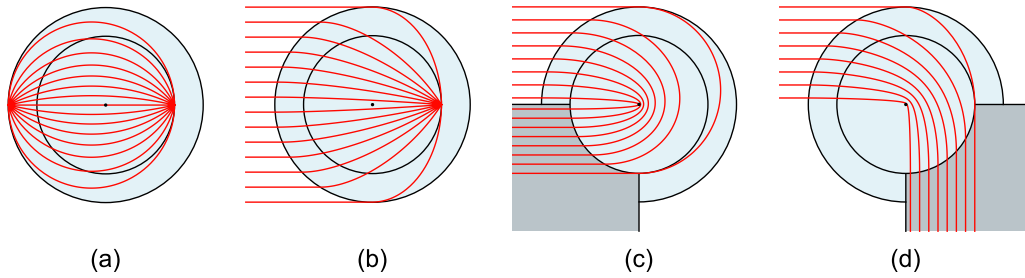


**Figure 12.** Ray tracing for several solutions of the generalized Luneburg problem: (a) Maxwell's fish-eye, (b) Gutman lens, (c) magnifying Eaton lens, (d) magnifying 90° rotating lens. The region of constant refractive index  $n_x$  is shown in darker blue.

**Table 2.** Solutions of the generalized Luneburg problem.

Lens	Refractive index
Maxwell's fish-eye	$n(r) = \frac{1+f^2}{f^2+r^2}$
Gutman (Luneburg)	$n(r) = \frac{1}{f}\sqrt{1+f^2-r^2}$
90° rotating	$f^2 m^4 - (1+f^2)n + r = 0$
Eaton	$n(r) = \frac{1}{f}\sqrt{\frac{1+f^2}{r} - 1}$
Invisible	$f^2 m^{3/2} + m^{1/2} - (1+f^2) = 0$

equivalent geodesic lens is a sphere. In the second example we choose  $A = B = \frac{1}{2}$  which gives us a Luneburg lens. As we know from section 2, the parallel rays starting from the unit circle are focused into the point on the same circle. Now, in addition, we also see that if we send light rays under the same angles from a circle of radius  $r_-(C)$ , they will be focused into the point on the circle of radius  $r_+(C)$ .

Obviously, by the property we have just described the geodesic lenses given by (24), in fact, represent the solution of the generalized Luneburg problem for special cases when  $r_1 \in \{1, \infty\}$  and  $r_2 \in \{r_x, \infty\}$ . To meet the boundary conditions specified at the beginning of this section we need to proceed in the following way. From geodesic lenses given by (24) we take only the part above the lower circle of chosen radius  $C$  and we rescale them, so that this circle becomes of unit radius. Then the equator has radius  $\rho_0 = 1/C$  and the functions that parametrize the geodesic lenses are

$$\begin{aligned} s_1(\rho) &= A\rho + BC^{-1} \arcsin C\rho & \rho &\in [0, \rho_0], \\ s_2(\rho) &= A\rho + BC^{-1}(\pi - \arcsin C\rho) & \rho &\in [1, \rho_0], \end{aligned} \quad (29)$$

where the domains of  $\rho$  are explicitly listed.

The calculation of the corresponding refractive index  $n(r)$  can be done in a similar way as in section 2.4. This time the condition  $\rho(1) = 1$  implies the relation

$$C = \frac{2f}{1+f^2} \quad (30)$$

between the scaling parameter  $C$  and the value  $f$  involved in the integration constant. Consequently, we find the equation

$$r^{2/B} - (1+f^2)r^{1/B}(nr)^{A/B-1} + f^2(nr)^{2A/B} = 0 \quad (31)$$

suitable for direct calculation of the refractive index from given  $A, B$  and  $f$ . Clearly, for  $f = 1$  this equation turns to (17). Moreover, it can be easily shown that (31) can be transformed to (17) by a simple substitution  $r \rightarrow rf^B/C^A$  and  $n \rightarrow nC^{A-1}/f^B$ . This means that the functions for refractive index obtained from (17) and (31) for given  $A, B$  can be mutually converted to each other by rescaling of the radial coordinate  $r$  and multiplying by a real positive constant (see table 2). In other words, the solutions of the generalized Luneburg problem do not represent fundamentally new functions for refractive indices, but utilize the previously unknown property of well-known refractive indices.

The examples of ray tracing for several combinations of  $A, B$  and  $f$  are shown in figure 12. For  $A = 0, B = 1$  we obtain a rescaled Maxwell's fish-eye whose imaging properties are well known. Choosing  $A = B = \frac{1}{2}$ , we come to the modification of the Luneburg lens which was first proposed by Gutman [13]. For  $A = B = 1$  we get a magnifying Eaton lens which has never been found before, as well as other lenses corresponding to other combinations of numbers  $A, B$ .

To summarize this section, we would like to emphasize that each of the found solutions of the generalized Luneburg problem is determined by a single formula for refractive index. This is in contrast to the solutions derived in [14, 15], where the refractive index is given by two different functions inside and outside the circle of radius  $r_x$ , on which the derivative of refractive index is discontinuous.

## 5. Conclusion

In this paper we studied spherical media using the concept of equivalent geodesic lenses. We found the general solution of the Luneburg inverse problem, and also a powerful method for designing and analyzing absolute instruments that provide perfect imaging within the frame of geometrical optics. Finally, we solved the generalized Luneburg problem which led to the discovery of a new class of lenses which utilize one previously unknown but very interesting property of well-known refractive indices.

## Acknowledgments

MŠ acknowledges support of the grant MUNI/A/0968/2009. TT acknowledges support of the grant P201/12/G028 of the

Grant agency of the Czech Republic and of the QUEST programme grant of the Engineering and Physical Sciences Research Council.

## References

- [1] Luneburg R K 1964 *Mathematical Theory of Optics* (Berkeley: University of California Press)
- [2] Eaton J E 1952 *Trans. IRE Antennas Propag.* **4** 66
- [3] Firsov O B 1953 *Zh. Eksp. Teor. Fiz.* **24** 279
- [4] Born M and Wolf E 2006 *Principles of optics* (Cambridge: Cambridge University Press)
- [5] Miñano J C 2006 *Opt. Express* **14** 9627
- [6] Tyc T, Herzánová L, Šarbort M and Bering K 2011 *New J. Phys.* **13** 033016
- [7] Rinehart R F 1948 *J. Appl. Phys.* **19** 860
- [8] Kunz K S 1954 *J. Appl. Phys.* **25** 642
- [9] Cornbleet S and Rinous P J 1981 *IEE Proc H* **128** 95
- [10] Sochacki J 1986 *Appl. Opt.* **25** 235
- [11] Berry M V 1975 *J. Phys. A: Math Gen.* **8** 1952
- [12] Miñano J C *et al* 2006 *Proc. Optical Design Conf. (Vancouver)* (Washington, DC: Optical Society of America) paper TuD4
- [13] Gutman A S 1954 *J. Appl. Phys.* **25** 855
- [14] Morgan S P 1958 *J. Appl. Phys.* **29** 1358
- [15] Tyc T 2011 *Phys. Rev. A* **84** 031801